Assessment of Conventional Density Functional Schemes for Computing the Dipole Moment and (Hyper)polarizabilities of Push−Pull π-Conjugated Systems†

ARTICLE *in* THE JOURNAL OF PHYSICAL CHEMISTRY A · APRIL 2000

Impact Factor: 2.69 · DOI: 10.1021/jp993839d

Assessment of Conventional Density Functional Schemes for Computing the Dipole Moment and (Hyper)polarizabilities of Push−Pull π-Conjugated Systems†

Benoît Champagne,* Eric A. Perpète, and Denis Jacquemin

Laboratoire de Chimie Théorique Appliquée, Facultés Universitaires Notre-Dame de la Paix, rue de Bruxelles, 61, B-5000 Namur, Belgium

Stan J. A. van Gisbergen and Evert-Jan Baerends

Section Theoretical Chemistry, Vrije Universiteit, De Boelelaan 1083, 1081 HV, Amsterdam, The Netherlands

Chirine Soubra-Ghaoui and Kathleen A. Robins

Department of Chemistry, University of Nevada, Las Vegas, Nevada 89154

Bernard Kirtman

Department of Chemistry, University of California, Santa Barbara, California 93106

Received: October 28, 1999; In Final Form: February 17, 2000

DFT schemes based on conventional exchange-correlation (XC) functionals have been employed to determine the dipole moment (μ), polarizability (α), and first (β) and second (γ) hyperpolarizabilities of push−pull π-conjugated systems. In addition to the failures already pointed out for α and γ in a recent study on polyacetylene chains [*J. Chem. Phys.* **1998**, *109*, 10489; *Phys. Rev. Lett.* **1999**, *83*, 694], these functionals are also unsuitable for the evaluation of μ and β. In the case of β, in particular, an almost catastrophic behavior with respect to increasing chain length is found. We show that the C functional has a negligible effect on the calculated μ, α, β, and γ whereas the X-part is responsible for the large property overestimations when the size of the system increases. The overly large μ values are associated with an overestimation of the charge transfer between the donor and the acceptor whereas for α, β, and γ, incomplete screening of the external electric field is responsible for the large discrepancies with respect to accurate values. Our results show that current XC functionals incorrectly describe the polarization of conjugated systems when the polarization is due to donor/acceptor substitution or an external field or both.

I. Introduction

Accurate quantum chemical evaluations of the polarizability (α), and first (β), and second (γ) hyperpolarizabilities are currently either beyond, or at, the borderline of what is feasible for large π-conjugated systems which are of interest for nonlinear optics (NLO). Although electron correlation can lead to substantial changes in the linear, and especially the nonlinear, response,[1] it is difficult to take into account. On the one hand, the computational requirements to perform classical Møller−Plesset (MP), configuration interaction (CI), coupled-cluster (CC), or multiconfigurational self-consistent field (MCSCF) calculations rapidly escalate with the size of the system. On the other hand, several papers have pointed out that density functional theory (DFT) based on current conventional exchange-correlation (XC) functionals fails drastically as regards the evaluation of field-response properties,[2−4] in contrast with ground state properties such as energies, geometries, and vibrational frequencies.

One can distinguish two periods of use of DFT for electric field response properties. First, due to its enormous success in determining field-independent properties, DFT was rapidly proposed for evaluating α, β, and γ. The first studies carried out on atoms and small molecules[5−13] were encouraging and led to the application of DFT to conjugated organic molecules.[14−18] In the last five years these developments have accelerated[19−39] and have concerned the use of improved XC functionals (nonlocal, hybrid, asymptotically correct, ...) as well as the treatment of frequency dispersion. A nice example of the present range of applicability of DFT methods for tackling materials science questions is the study of buckminsterfullerene.[28] However, much has still to be done for both small and large molecules. For computing α several functionals are of similar performance (at least) to more sophisticated post-Hartree−Fock methods,[20,23,31,36,38−39] but the situation for the first and second hyperpolarizabilities is not as clear.[30,33,37] It is not unusual that the common local and nonlocal XC functionals will overestimate β and γ, assuming a sufficiently extended basis set, and that including the correct asymptotic $-1/R$ behavior of the XC potential will not always yield a value better than Hartree−Fock. Nevertheless, a very recent improvement in the modeling of the XC potentials shows promise in the calculation of better hyperpolarizabilities for small molecules.[39]

Although refinement of the XC functional improves the hyperpolarizability values for small molecules, we have recently demonstrated that, in the case of polyacetylene oligomers, DFT

* Corresponding author.

† Part of the special issue "Electronic and Nonlinear Optical Materials: Theory and Modeling".

10.1021/jp993839d CCC: $19.00
Published on Web 04/12/2000

schemes based on conventional and less conventional XC functionals fail in one or more of several ways:[2−4] (i) the correlation correction to α is either much too small or in the wrong direction, leading to an overestimation with respect to usual post HF methods; (ii) γ is significantly overestimated; (iii) the chain length dependence is excessively large, particularly for γ and for the more alternant systems; and (iv) the bond length alternation (BLA) effects upon γ are qualitatively incorrect such that the γ vs BLA curve presents a maximum. Since no improvements were obtained with the asymptotically correct van Leeuwen−Baerends XC potential,[40] the overestimations are unrelated to the poor asymptotic behavior. Instead, these failures have been related to the short-sightedness of the XC potentials which do not adequately screen the polarization charge induced by the external electric field at the chain ends. This has been traced[3] to an incorrect electric field dependence of the response part of the XC potential which, contrary to the exact XC potential as well as the Hartree−Fock and post-Hartree−Fock treatments, lacks a linear term counteracting the applied electric field. The exchange-only Krieger−Li−Iafrate (KLI) potential (based on the Kohn−Sham orbitals instead of the total density)[41] clearly exhibits this counteracting term. Apart from the fact that it only models exchange, the KLI potential has the drawback that it is expensive to calculate thereby precluding its application to large molecules. Another approach to curing the XC functional is through polarization-dependent density functional theory (PDDFT) which consists of adding a polarization-dependent term (linear in the field amplitude) to the XC functional.[42]

For extended systems other than prototype polyacetylene chains, the appropriateness of conventional local and nonlocal density functionals for computing α, β, and γ remains an open question. Push−pull π conjugated molecules are especially interesting in this regard because of potential applications and the fact that they possess both first and second hyperpolarizabilities. In this study of some prototypical push−pull molecules (*p*-nitroaniline = PNA, 4-amino-4′-nitrostilbene = ANS, $NH_2(CH{=}CH)_6NO_2$ = N6, and $NH_2(CH{=}CH)_{12}NO_2$ = N12), we document the failure of conventional DFT for μ and β as well as α and γ. An initial analysis is carried out which identifies the source of the discrepancy as far as the functional is concerned and from a physical perspective. It is hoped that this will lead to both fundamental (better XC functionals) and practical (identification of problematic systems and properties) improvements.

The next section gives a brief account of the methods we have employed, i.e., the different DFT schemes as well as the various techniques to evaluate μ, α, β, and γ. The results are then given for μ and β, which have not been studied before in this context, and, then, for α and γ, which were examined in our related investigation of PA chains.[2−4] The abilities and failures of conventional DFT functionals to include electron correlation effects on these *electrical* properties are considered as a function of the system size and they are analyzed by considering field-induced charge patterns.

II. Methodology and Computational Procedure

In DFT, the electron density is the central quantity which solely determines all the system properties.[43−44] It is usually evaluated self-consistently by solving the Kohn−Sham equation which involves kinetic, Coulombic, exchange, and correlation terms. The quality of the results depends on the choice of the XC functional.

In this work, we have employed different XC functionals starting with the local density approximation (LDA) and improving it with the inclusion of gradient corrections and correct asymptotic behavior. This first XC functional, denoted SVWN, is composed of the local Slater exchange functional (S)[45] plus the uniform electron gas local correlation functional due to Vosko, Wilk, and Nusair (VWN).[46] It can be improved by including gradient corrections for exchange, by means of Becke's (B),[47] Perdew and Wang's (PW91),[48] or Gill's (G96)[49] expressions, and for correlation by adopting the Lee, Yang, and Parr (LYP)[50] or the Perdew and Wang (PW91)[48] functionals. Thus, SLYP, SPW91, and BVWN include nonlocal corrections for either the correlation or exchange functionals whereas BLYP, BPW91, PW91PW91, and G96LYP incorporate nonlocal corrections in both terms. In the three-parameter B3LYP functional,[51] the exchange potential includes some percentage of the exact HF exchange, the remaining part being described by the Slater functional plus a weighted Becke gradient correction. In Gaussian94/Gaussian98,[52,53] the standard formula is to replace 20% of DFT exchange by HF exchange [B3LYP = B3LYP (20%)] but we have also considered a 50% [B3LYP′ (50%)] and an 80% [B3LYP″ (80%)] replacement in order to distinguish between the effects of the HF and DFT exchange functionals. The correlation part of the B3LYP functional includes a weighted combination of the local VWN and nonlocal LYP correlation potentials. Another hybrid scheme, *m*PW1PW91, has also been examined: it is a one-parameter functional combining HF exchange, modified Perdew−Wang exchange, and Perdew−Wang 91 correlation.[54] Of comparable quality to B3LYP for covalent interactions, this functional has also been shown to be significantly better for noncovalent interactions. Following our first investigation of PA chains,[2] we have also addressed the significance of the correlation correction within the DFT scheme by combining HF exchange with either the VWN or the LYP functional giving rise to the HFVWN and HFLYP methods. Further comments about this splitting of the XC functional can be found in ref 2. For all the DFT methods described above, the Gaussian94/Gaussian98 programs[52,53] have been utilized with different Gaussian-type atomic basis sets.

Additional DFT calculations were carried out with the response module[55] of the Amsterdam density functional (ADF) program[56] using Slater-type orbitals and a density fitting procedure for the Coulomb-type integrals based on auxiliary basis functions. The ADF calculations were performed with five different sets of XC functionals and kernels. The XC kernels, which are the first or higher functional derivatives of the XC potential with respect to the density, enter explicitly into the evaluation of α and β in the ADF code. One scheme consists of using a local density approximation (LDA) for both the potential and kernel. It can be labeled LDA/LDA and is identical to the SVWN approach mentioned above, except for differences in basis sets or numerical precision. These functionals can be improved by using the asymptotically correct van Leeuwen−Baerends (LB94) XC potential[40] in the LB94/LDA procedure and further by using the LB94 expressions for both the potential and kernels (LB94/LB94). The latter leads to results which are equivalent to those from a finite field LB94 calculation. The mixed LB94/LDA scheme, which cannot be obtained from a FF approach, has been highlighted as a better method for computing linear and nonlinear optical properties of small molecules.[23,29] Two other schemes that were not applied in ref 2 are employed here. One of them adds a nonlocal XC correction with the functional of Becke[47] and Perdew[57] (BP86) to get the mixed BP86/LDA scheme. The other consists of the new XC potential[39] based on statistical averaging of (model) orbital potentials (SAOP). This potential has recently been shown to

yield improved estimates of β and γ, as well as excitation energies for prototype molecules such as N_2, C_2H_4, and CO in comparison with the LDA and LB94 potentials.

When a static homogeneous external electric field is applied along the longitudinal axis of a molecule, it induces a dipole moment having the longitudinal component:

$$\Delta\mu_L(F) = \alpha_L F + \frac{1}{2}\beta_L F^2 + \frac{1}{6}\gamma_L F^3 + ... \quad (1)$$

where α_L, β_L, and γ_L include both electronic and vibrational contributions. As a result of electron delocalization along the backbone, the longitudinal component is by far the largest in extended systems such as push−pull π-conjugated molecules. The DFT failures are associated with the longitudinal extension and is another reason for restricting our study to this component. Although the vibrational contribution can be substantial for many NLO processes,[58] this work focuses on the static electronic contribution and we denote the longitudinal tensor component simply by α, β, and γ.

In Gaussian94/Gaussian98,[52,53] the coupled-perturbed Kohn−Sham (CPKS) technique[59] is adopted for computing α whereas in ADF the equivalent linear response equations of time-dependent density functional theory (TDDFT)[60] are solved in the static limit. The latter procedure also provides β via the use of the $2n + 1$ rule.[32] The higher-order properties (β and γ at the CPKS and γ at the TDDFT levels) were obtained by a finite field (FF) procedure where α or β is evaluated at different field amplitudes:

$$\beta^{0,k} = \frac{\alpha(2^kF) - \alpha(-2^kF)}{2^{k+1}F} \quad (2)$$

$$\gamma^{0,k} = \frac{[\alpha(2^kF) + \alpha(-2^kF) - 2\alpha(0)]}{(2^kF)^2} = \frac{\beta(2^kF) - \beta(-2^kF)}{2^{k+1}F} \quad (3)$$

with $k \geq 0$. Accurate first- and second-order derivatives require that the field amplitude be small enough to avoid contaminations from the higher-order hyperpolarizabilities. However, the smaller the field amplitude, the lower the accuracy of γ because the number of significant digits in the field-dependent (hyper)-polarizability difference decreases. A good compromise was found by taking $F = 0.0004$ au, $k = 0-5$ for the smaller systems and $F = 0.000\,012\,5$ au, $k = 0-6$ for the larger systems while simultaneously employing a Romberg type procedure[61] to remove the higher-order contaminations. These successive improvements of the $\beta(\gamma)$ estimates from the initial $\beta^{0,k}(\gamma^{0,k})$ values were calculated using the general iterative expression:

$$\beta^{p,k} = \frac{4^p\beta^{p-1,k} - \beta^{p-1,k+1}}{4^p - 1} \quad (4)$$

where p is the order of the Romberg iteration. This procedure results in an accuracy of 0.01−0.5% in β and γ. In order to reach this accuracy, it was found sufficient in the Gaussian94/Gaussian98 calculations to adopt the Lebedev integration scheme with 75 radial points and 302 angular points.

For comparison purposes, the Hartree−Fock as well as the Møller−Plesset technique limited to second (MP2) and fourth (MP4) order in electron correlation were also used to determine these properties. At the HF level, the evaluation of α is performed through the coupled-perturbed Hartree−Fock (CPHF) procedure[62] and a similar FF scheme (eqs 2−4) is adopted to determine β and γ. At the MPn levels ($n = 2, 4$), we employ an equivalent FF procedure based either on the polarizability or, for large systems (substituted polyenes and ANS), on the successive energy derivatives:

$$\alpha^{0,k} = -\frac{[E(2^kF) + E(-2^kF)] - 2E(0)}{(2^kF)^2}$$

$$\beta^{0,k} = -\frac{[E(2^{k+1}F) - E(-2^{k+1}F)] - 2[E(2^kF) - E(-2^kF)]}{2(2^kF)^3}$$

$$\gamma^{0,k} = -\frac{[E(2^{k+1}F) + E(-2^{k+1}F)] - 4[E(2^kF) + E(-2^kF)] + 6E(0)}{(2^kF)^4} \quad (5)$$

In order to reach the precision given above, the Romberg procedure with $F = 0.0008$ au, $k = 0-4$, was utilized for the smaller systems and $F = 0.0001$ au, $k = 0-7$, for the larger systems. At the same time, it was necessary to tighten the threshold on the HF energy in the SCF procedure to 10^{-12} au.

The dipole moment, μ, was obtained from the usual expectation value expression with the exception of the MP2 and MP4 levels where it was evaluated as the negative of the first derivative of the energy with respect to the applied field. These FF-derived MP2 μ values agree within less than 0.1% with the values determined from the GAUSSIAN MP2 density.

The calculations carried out with the Gaussian94/Gausian98 program used the split-valence 6-31G basis set.[63] To address the accuracy with respect to the basis set, we have also performed calculations with the 6-31G basis augmented by a set of diffuse P and D functions on the non-hydrogen atoms. Similar studies have shown that the 6-31G basis set is adequate for computing accurate electronic (hyper)polarizabilities of extended π-conjugated oligomers.[64−65] In the ADF calculations, double-ζ (DZ) Slater-type orbitals basis sets from the standard ADF basis set database along with the corresponding auxiliary basis were employed[66] as well as triple-ζ with one (TZ+P) or with two (TZ+2P) polarization functions basis sets. Additionally, some calculations were performed where diffuse functions were added to the TZ+2P ADF basis set.

III. Results and Discussion

Four molecules were used to assess the ability of a large range of DFT XC functionals. These molecules include two α,ω-nitroaminopolyenes containing six and 12 CH=CH units referred to as N6 and N12 as well as *p*-nitroaniline (PNA) and 4-amino-4′-nitrostilbene (ANS). From the viewpoint of NLO devices the latter are more realistic compounds because they are easily tractable and stable (see Scheme 1).

The geometries of PNA and ANS were completely optimized at the RHF/6-31G level of approximation whereas, for the substituted polyenes, we were able to use fully optimized MP2/6-31G geometries taken from a separate investigation.[67] In the case of PNA, the longitudinal axis obviously contains the substituted carbon atoms that are para to one another. For ANS and the substituted polyenes the corresponding inertial axis was chosen. In all instances the longitudinal axis is essentially parallel to the dipole moment. The calculated μ, α, β, and γ values for these four molecules are given in Tables 1−4.

III.A. Dipole Moment and First Hyperpolarizability. For all the molecules the effect of electron correlation, as determined by MP2 and MP4 (in the case of PNA and ANS), is to lower the dipole moment. On the other hand, the DFT schemes we have tried either increase μ or do not alter it significantly from

SCHEME 1: Representation and Acronyms of the Four Molecules

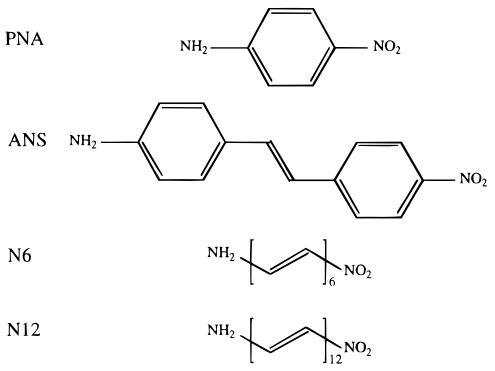

TABLE 1: Longitudinal Component of the Electronic Dipole Moment, Static Polarizability, First Hyperpolarizability, and Second Hyperpolarizability of *p*-Nitroaniline Obtained by the CHF, MP2, and Various DFT Methods[a]

	μ	α	β	γ (10^2 au)
		6-31G		
MP2	2.78	128.6	1931	1337
MP4	2.78	127.7	1943	1422
RHF	3.23	118.7	1263	709
S	3.15	144.4	1596	352
B	3.08	143.2	1637	407
HFVWN	3.29	118.4	1305	730
HFLYP	3.27	118.8	1300	727
SVWN	3.23	144.3	1650	303
SLYP	3.20	144.5	1613	311
BVWN	3.16	143.1	1691	362
BLYP	3.14	143.4	1656	366
B3LYP (20%)	3.15	137.0	1698	612
B3LYP′ (50%)	3.17	128.8	1594	778
B3LYP″ (80%)	3.22	122.3	1422	775
		6-31G+PD		
MP2	2.81	150.8	2323	1968
CHF	3.19	133.4	1420	985
SVWN	3.30	168.1	2005	675
BLYP	3.23	168.9	2053	796
B3LYP (20%)	3.20	158.9	2060	1054
		DZ		
LDA/LDA	3.56	146.2	1749	298
LB94/LDA	3.76	152.9	1812	11
		TZ+P		
LDA/LDA	3.18	161.6	1781	464
LB94/LDA	3.41	167.4	1911	176
		TZ+2P		
LDA/LDA	3.18	161.4	1762	485
LB94/LDA	3.41	167.3	1903	193
BP86/LDA	3.12	158.9	1735	507
SAOP/LDA	3.45	160.8	1774	298
		TZ+2P+Diffuse		
LDA/LDA	3.12	170.1	1720	774

[a] Unless specified, all values are in atomic units (1.0 au of dipole moment = $8.478\,358 \times 10^{-30}$ C m = 2.541 76 D; 1.0 au of polarizability = 1.6488×10^{-41} C^2 m^2 J^{-1} = 0.148 18 Å^3; 1.0 au of first hyperpolarizability = 3.2063×10^{-53} C^3 m^3 J^{-2} = 8.641×10^{-33} esu; 1.0 au of second hyperpolarizability = $6.235\,377 \times 10^{-65}$ C^4 m^4 J^{-3} = 5.0367×10^{-40} esu). The RHF/6-31G geometry is used in all cases.

the Hartree−Fock value. The fact that the MP2 and MP4 values are close to one another, and that CCSD and CCSD(T) results on shorter ($N = 1-2$) substituted polyenes yield values similar to MP2,[68] tends to confirm our conclusion that conventional XC functionals fail for this problem. From Tables 1−4 it is evident that this conclusion is basis set independent and, as we have found previously for α and γ the DFT error increases as the molecule is lengthened (cf. Tables 3 and 4). Our results for PNA are similar to those obtained by Sim et al.[69] In contrast with previous failures for α, β, and γ, which are due to the dipole induced by an external field, in this case we are dealing with a permanent property of the unperturbed molecule. An analysis of the variations of μ as a function of the XC functional shows that the increase with respect to the Hartree−Fock value is connected to the X term. The C term, on the other hand, should lead to a substantial reduction in μ but only has a minor effect. In support of these statements, we note that (i) including correlation effects by using local and nonlocal C functionals with the exact HF exchange (HFVWN and HFLYP) changes the RHF values by less than 2%; (ii) similarly, a comparison of SVWN and SLYP with S (or the same with B instead of S) shows little effect of adding the C functional; (iii) replacing HF exchange by Slater or Becke exchange (e.g., HFVWN → SVWN) leads to a large increase in μ; and (iv) tuning the percentage of HF/DFT exchange within the B3LYP hybrid scheme results in an almost monotonic decrease from the BLYP to the RHF value as a function of the decreasing percentage of DFT exchange. The fact that the *m*PW1PW91 XC functional gives values close to B3LYP is undoubtedly related to its amount of HF exchange: 25%. Finally, the role of nonlocal corrections is insignificant. This may be deduced from the fact that adding nonlocal corrections to the X functional (BVWN), to the C functional (SLYP) or to both (BLYP, BPW91, PW91PW91, and G96LYP) brings negligible modification to the SVWN values.

The LDA/LDA results found with the ADF program are close to those obtained with GAUSSIAN at the SVWN level. This is

TABLE 2: Longitudinal Component of the Electronic Dipole Moment, Static Polarizability, First Hyperpolarizability, and Second Hyperpolarizability of 4-Amino-4′-nitrostilbene Obtained by the CHF, MP2, and Various DFT Methods[a]

	μ	α	β	γ (10^3 au)
		6-31G		
MP2	3.16	342.1	10110	2072
MP4	3.18	336.9	10190	2184
RHF	3.88	332.7	6339	1023
S	4.21	503.2	27829	4886
B	4.11	495.1	27414	5160
HFVWN	3.92	332.0	6485	1049
HFLYP	3.94	331.2	6429	1033
SVWN	4.29	505.9	29298	4988
SLYP	4.29	506.7	28711	4859
BVWN	4.20	497.7	28862	5303
BLYP	4.29	498.7	28349	5165
*m*PW1PW91	3.99	424.5	18427	3988
B3LYP (20%)	4.01	437.0	20153	4363
B3LYP′ (50%)	3.88	379.1	12008	2415
B3LYP″ (80%)	3.60	340.0	8009	1410
		DZ		
LDA/LDA	4.24	517.3	32673	5229
LB94/LDA	4.60	560.8	38786	3754
		TZ+P		
LDA/LDA	4.25	543.6	29967	5331
LB94/LDA	4.61	583.0	36907	4700
LB94/LB94	4.61	565.9	3492×10	42×10^2
		TZ+2P		
LDA/LDA	4.24	541.7	29537	5342
LB94/LDA	4.60	581.4	36695	4856
BP86/LDA	4.16	531.0	28472	5538
SAOP/LDA	4.62	548.7	31240	4470

[a] Except where specified, all values are in atomic units. The RHF/6-31G geometry is used in all cases.

TABLE 3: Longitudinal Component of the Electronic Dipole Moment, Static Polarizability, First Hyperpolarizability, and Second Hyperpolarizability of $NH_2(CH{=}CH)_6NO_2$ Obtained by the CHF, MP2, and Various DFT Methods[a]

	μ	α	β (10 au)	γ (10^4 au)
		6-31G		
MP2	4.03	665.5	6266	1799
RHF	5.87	734.9	2845	654
S	6.77	1059.7	4602	213
B	6.62	1053.1	4689	279
HFVWN	5.96	734.8	2860	654
HFLYP	5.91	733.8	2937	677
SVWN	6.91	1064.9	4709	162
SLYP	6.88	1063.7	4628	173
BVWN	6.76	1058.1	4793	234
BLYP	6.73	1057.4	4714	236
BPW91	6.78	1058.3	4752	225
PW91PW91	6.76	1057.5	4739	231
G96LYP	6.78	1060.2	4721	230
MPW1PW91	6.34	955.1	5563	844
B3LYP (20%)	6.40	976.1	5471	730
B3LYP′ (50%)	6.02	853.6	4908	1060
B3LYP″ (80%)	5.82	767.3	3553	835
		DZ		
LDA/LDA	7.36	1088.2	4972	86
LB94/LDA	7.91	1138.8	4947	195
		TZ+2P		
LDA/LDA	6.81	1124.0	4961	298
LB94/LDA	7.38	1180.0	5204	

[a] Except where specified, all values are in atomic units. The MP2/6-31G geometry is used in all cases.

TABLE 4: Longitudinal Component of the Electronic Dipole Moment, Static Polarizability, First Hyperpolarizability, and Second Hyperpolarizability of $NH_2(CH{=}CH)_{12}NO_2$ Obtained by the CHF, MP2, and Various DFT Methods[a]

	μ	α	β (10^3 au)	γ (10^5 au)
		6-31G		
MP2	4.18	1504.7	184	136 × 10
RHF	6.73	2004.4	101	622
S	9.84	4291.8	656	220 × 10
B	9.56	4235.0	665	258 × 10
HFVWN	6.83	1997.0	100	606
HFLYP	6.76	1989.6	103	627
SVWN	10.03	4315.9	682	216 × 10
SLYP	10.00	4317.1	665	221 × 10
BVWN	9.75	4257.1	693	267 × 10
BLYP	9.73	4261.9	677	254 × 10
B3LYP (20%)	8.50	3467.2	611	449 × 10
B3LYP′ (50%)	7.29	2558.2	290	224 × 10
B3LYP″ (80%)	6.76	2131.6	143	951
		DZ		
LDA/LDA	10.63	4417.2	735	205 × 10
LB94/LDA	11.59	4683.2	790	595
		TZ+2P		
LDA/LDA	9.86	4466.1	690	272 × 10
LB94/LDA	10.84	4749	784	155 × 10

[a] Except where specified, all values are in atomic units. The MP2/6-31G geometry is used in all cases.

especially true when the basis sets are reduced in size due to system extent. The use of the LB94 XC functional with the correct asymptotic behavior does not improve the DFT estimates. The SAOP potential which, apart from the correct asymptotic behavior, is superior to LDA in the inner molecular region (at least, for small molecules) also does not lead to improved results. This suggests that rather special features in the XC functionals are required to correct the LDA values in agreement with the analysis of refs 2−4.

DFT fails for β in a somewhat different way than for μ. Calculations at the MP2 and MP4 level show a large increase in this property value compared with results at the RHF level. From Table 1 we see that the % increase is not affected (at least, in the case of PNA) by increasing the size of the basis. For the substituted polyenes a few calculations have been carried out elsewhere[65] for the smallest chains at the CCSD and CCSD(T) levels of approximation. The difference in β with respect to the MP2 value was found to be always smaller than 6%. Common XC functionals also give rise to an increase of β with respect to the CHF values but it is either too small for the smallest system of each class (i.e., PNA, N6) or much too large for the largest compounds (ANS, N12). Obviously, the dependence of β on system size is exaggerated by DFT levels as it is for α and γ of unsubstituted polyenes.[2−4] Again, the variation in the DFT value of β is closely connected to the amount of HF exchange whereas the correlation functional has a negligible impact. We also point out the improved, although probably fortuitous, behavior of the hybrid functionals for N6. As before, (i) the LDA/LDA results are very close to the SVWN GAUSSIAN values; (ii) insisting on the correct asymptotic behavior (LB94/LDA, LB94/LB94) is not important; and (iii) the new SAOP potential does not improve the results.

In order to further address size effects, we have investigated α,ω-nitroaminopolyenes of increasing length with the SVWN and B3LYP functionals as well as with the reference RHF and MP2 techniques. The RHF and MP2 values have been taken from ref 67. As a result of the competition between asymmetry and delocalization, the first hyperpolarizability per unit cell (or per unit length or volume) β/N exhibits a maximum for a chain containing $N = 10-15$ CH=CH units and tends asymptotically toward zero.[67,70] The asymptotic behavior of β/N is a reflection of the fact that the effect of substitution is more or less localized to the chain ends and, hence, β will saturate as N approaches infinity. A knowledge of the chain length associated with the maximum β/N value is critical for optimizing the second-order NLO response of a material. Figure 1a displays the chain length dependence of $\beta(N)/N$ where N is the number of unit cells. Although the MP2 values are a factor of 2 larger than HF, both curves are similar in shape with a maximum appearing for $N = 14$ (HF) and $N = 12$ (MP2) corresponding to β/N values of 860 × 10 and 1528 × 10 au, respectively. On the other hand, the SVWN and B3LYP curves are still increasing rapidly for $N = 14$ and the corresponding values of β/N are at least 1 order of magnitude larger than MP2 and RHF. Because B3LYP contains 20% Hartree−Fock exchange, it behaves somewhat better than SVWN but both curves show an almost "catastrophic" increase with N. From Figure 1a it is impossible to determine whether the DFT calculations will exhibit a maximum. In order to answer this question, we decided to perform calculations with the minimal STO-3G basis set. The geometries were optimized with the Austin model 1 (AM1) semiempirical scheme and in this way we were able to investigate chains containing up to 30 CH=CH unit cells. It turns out that there is a maximum in the SVWN β/N, although (at the STO-3G/AM1 level) the chain length is roughly twice as long as it should be and the value of β/N is about 2 orders of magnitude too large.

A similar study of the chain length dependence was carried out for μ which, like β, should tend toward a constant value when the system size increases (Figure 2). As we have already seen for $N = 6$ and 12, conventional DFT functionals overestimate μ. This is true at all N; for $N > 4$ the DFT values are worse than Hartree−Fock. In comparison to MP2 the saturation

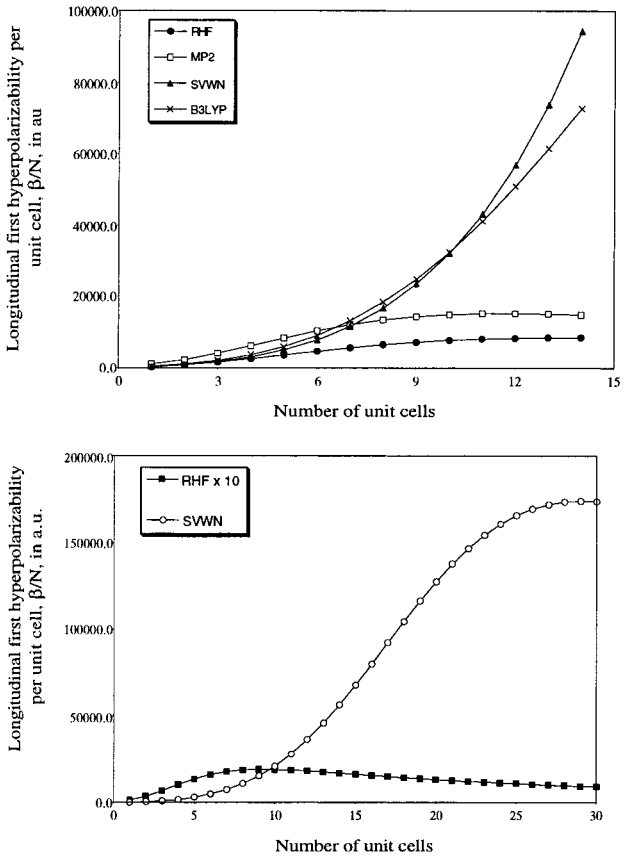

Figure 1. Evolution of the longitudinal first hyperpolarizability per unit cell, $\beta_L(N)/N$, of $NH_2(CH{=}CH)_NNO_2$ as a function of the number, N, of CH=CH units for different methods: (a, top) MP2/6-31G geometry and 6-31G properties; (b, bottom) AM1 geometry with STO-3G properties (RHF values multiplied by a factor of 10).

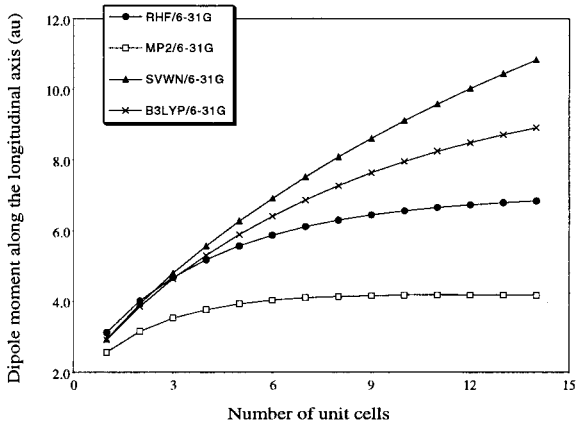

Figure 2. Evolution of the longitudinal dipole moment of NH_2-$(CH{=}CH)_NNO_2$ as a function of the number (N) of CH=CH units for different methods.

with chain length is slower and the limiting values are more than 2 (B3LYP) or 3 (SVWN) times larger. These results can be related to our previous study on unsubstituted polyenes[2−4] assuming it is *qualitatively* correct to say that the D/A pair plays a role similar to an external electric field.[71] In that event μ(substituted polyene) will be proportional to α(unsubstituted chain) and to the field created by the D/A pair. An analogous relation holds between β(substituted polyene) and γ(unsubstituted chain). Thus, the behavior of μ (β) for the D/A chains will qualitatively parallel that of α (γ) for the unsubstituted polyenes. This is consistent with (1) a decrease in μ upon including electron correlation at the MP2 level as opposed to

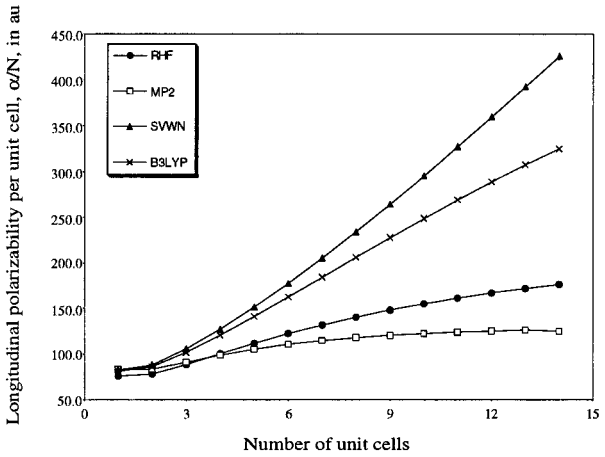

Figure 3. Evolution of the longitudinal polarizability per unit cell, $\alpha_L(N)/N$, of $NH_2(CH{=}CH)_NNO_2$ as a function of the number, N, of CH=CH units for different methods.

little change (for short chains) or a substantial increase using DFT; and (2) an increase in β upon including correlation at the MP2 level as compared to a smaller increase for DFT (SVWN and B3LYP) at short chain lengths but a much larger increase for long chains.

III.B. Polarizability and Second Hyperpolarizability. For α, including electron correlation at the MP2 level may lead either to an increase (PNA, ANS) or a decrease (N6, N12) but the effect is small compared to the large increase found in conventional DFT calculations. On the other hand, the MP2 γ is always much larger than the CHF value. In comparison, our DFT results for γ show a substantial decrease (with respect to CHF) for the shorter molecule (PNA, N6) of each type and a very large overestimate vs MP2 for the longer molecule (ANS, N12). The difference between MP4 and MP2 in Tables 1 and 2 is relatively small for both α and γ. Although these 6-31G results are underestimated with respect to those obtained with a basis set augmented by diffuse functions (mainly γ), the relationship between the various methods remains essentially unchanged. As in the case of μ and β, our results are in close agreement with those of Sim et al.[69] for PNA provided one takes into account the difference of conventions in the definitions of β and γ.

An analysis of the DFT results for α and γ reveals that, in most respects, they behave much like μ and β. In either case, the change with respect to Hartree−Fock is primarily determined by the X term and the role of nonlocal corrections is insignificant (although, for γ the difference between Slater and Becke exchange is not completely negligible). When one increases the amount of HF exchange in the B3LYP functional, the properties evolve from the BLYP to the HFLYP $\approx$ RHF value. This evolution is monotonic, as before, except for the γ value of the short chain of each type (PNA, N6) which exhibits a maximum. The LDA/LDA results from the ADF program are close to those obtained with GAUSSIAN at the SVWN level. Again, neither the LB94 or SAOP functionals, which have the correct asymptotic behavior, significantly improve the estimates. The one exception to this, i.e., γ of N12, appears to be a fortunate coincidence. Figure 3 confirms the failure of the SVWN and B3LYP functionals to describe properly the chain length dependence of α in the case of increasingly large α,ω-nitroaminopolyenes. Note that deviations from RHF are in the wrong direction compared to MP2 and that the errors are magnified when the chain length increases.

III.C. Charges and Induced Charges Analysis. In order to investigate the charge distribution induced by the D/A pair along

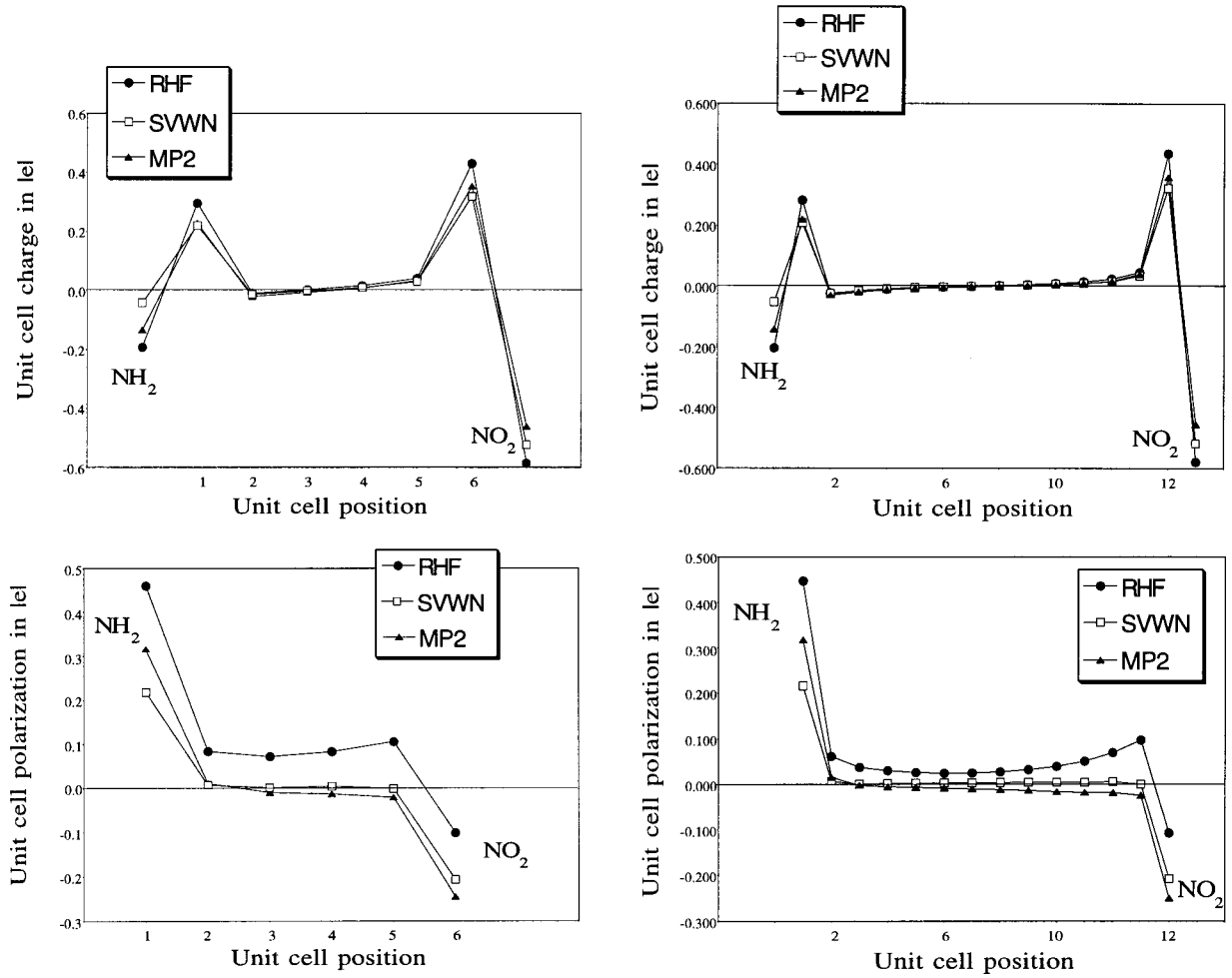

Figure 4. (top) Total charge per C_2H_2 unit cell and (bottom) polarization charge within each C_2H_2 unit cell as a function of position along the $NH_2(CH{=}CH)_6NO_2$ (left) and $NH_2(CH{=}CH)_{14}NO_2$ (right) backbone computed as described in the text using a 6-31G basis set.

the polyene backbone a Mulliken population analysis has been utilized. This was carried out by using the Gaussian94 program.[52] We realize that the Mulliken procedure is not suitable for a quantitative treatment. Our intent here is to describe only *qualitative* differences between DFT (SVWN) on the one hand and RHF or MP2 on the other. Figure 4 displays both the unit cell charge and the charge polarization within the unit cell as a function of the position along the backbone in the N6 and N14 chains. The meaning of unit cell charge is obvious; the charge polarization within the unit cell corresponds to the difference of charges on the two constituent CH groups.

The picture to bear in mind is that of a local dipole pointing in opposite directions at either end of the chain. These dipoles are created by transfer of charge along the backbone (i.e., the polyene linker). From Figure 4 the unit cell charge distributions are similar in all three cases. Nevertheless, a revealing distinction is obtained if one sums the charges separately on either side of the molecule. In doing so we note that the central unit cell bears a negligible charge. For N6, the half-chain charges are 0.097 |e|, 0.073 |e| and 0.164 |e|, for RHF, MP2, and SVWN respectively, with the positive charge being on the NH_2 side as expected. This correlates well with the trend in the μ values. For N14, the half-chain charges become smaller—0.034 |e|, 0.014 |e|, and 0.111 |e|—corresponding to a decreased charge transfer. Therefore, the overestimation of the dipole moment obtained with conventional XC functionals is associated with excessive charge transfer between the donor and acceptor. On the other hand, the unit cell charge polarization appears to be fairly well determined by the SVWN functional in the sense that the latter agrees more closely with MP2 than with RHF.

We continue *our* charge distribution analysis by plotting the *field-induced* unit cell charges and *field-induced* unit cell charge polarization for N6 in Figure 5. Here the electric field has an amplitude of 0.0020 au and is directed along the NO_2-NH_2 axis such that electron density is transferred from the donor to the acceptor. The field-induced unit cell charges obtained for SVWN differ from the RHF and MP2 patterns. In the SVWN approach, larger charges are found at the chain ends and the gradient across the chain is also larger. When the field is applied in the reverse direction, the induced unit cell charges are of opposite sign but a similar picture is obtained. These features can be associated with incomplete screening of the field due to the short-sightedness of the XC functional which does not contain (as it should) a counteracting linear field term.[3] A similar picture was found in our earlier work on unsubstituted polyene chains.[2,4] On the other hand, the field-induced unit cell polarization obtained with SVWN is more nearly like MP2 than RHF in agreement with the results given above for the D/A substituent effect.

IV. Conclusion

DFT schemes based on conventional exchange-correlation (XC) functionals have been employed to determine μ, α, β, and γ of push−pull π-conjugated systems. In addition to the failures already pointed out for α and γ in a recent study on polyacetylene chains,[2−4] we find that conventional functionals are also

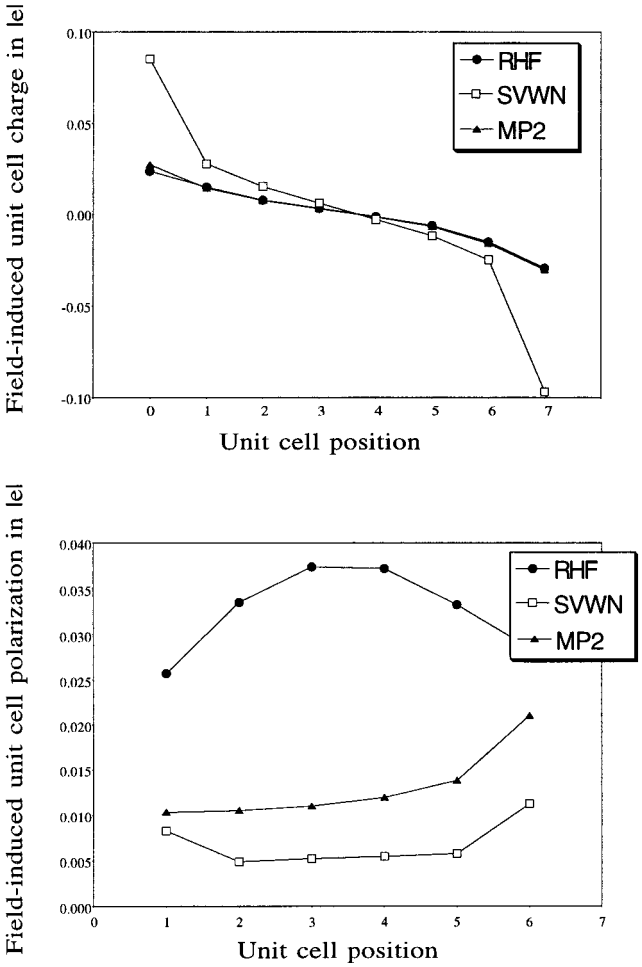

Figure 5. (top) Field-induced unit cell charges and (bottom) field-induced unit cell polarization charges as a function of the unit cell position along the $NH_2(CH{=}CH)_6NO_2$ backbone computed as described in the text using a 6-31G basis set. The electric field has an amplitude of 0.0020 au and is directed along the NO_2-NH_2 axis such that electron density is transferred from the donor to the acceptor.

unsuitable for the evaluation of μ and β when donor/acceptor substituents are added at the chain ends. In the case of β, in particular, a nearly catastrophic behavior with respect to increasing chain length is obtained. An analysis of the failures in terms of the separate effects of the X and C functionals shows that the C functional has a negligible effect on μ, α, β, and γ whereas the X part is responsible for the large property overestimations when the size of the systems increases. The overly large μ values have been associated with excessive charge transfer between the donor and the acceptor whereas for α, β, and γ incomplete screening of the external electric field is responsible for the large errors.

Acknowledgment. B.C. and E.A.P thank the Belgian National Fund for Scientific Research for their Research Associate and Postdoctoral Researcher positions, respectively. Calculations were performed on the IBM SP2 of the Namur Scientific Computing Facility (Namur-SCF), on the IBM SP2 of the Stichting Academisch Rekencentrum Amsterdam (SARA), as well as using the W.M. Keck Computational Physics Laboratory (UNLV). B.C., E.A.P, and D.J. gratefully acknowledge the financial support of the FNRS-FRFC, the Loterie Nationale for the convention No. 2.4519.97 and the Belgian National Interuniversity Research Program on Sciences of Interfacial and Mesoscopic Structures (PAI/IUAP No. P4/10). C.S.G. thanks the NSF-EPSCoR for financial support.

References and Notes

(1) Maroulis, G.; Thakkar, A. J. *J. Chem. Phys.* **1991**, *95*, 9060. Sim, F.; Chin, S.; Dupuis, M.; Rice, J. E. *J. Phys. Chem.* **1993**, *97*, 1158. Jaszunski, M.; Jørgensen, P.; Koch, H.; Ågren, H.; Helgaker, T. *J. Chem. Phys.* **1993**, *98*, 7229. Toto, J. L.; Toto, T. T.; de Melo, C. P.; Hasan, M.; Kirtman, B. *Chem. Phys. Lett.* **1995**, *244*, 59. Toto, J. L.; Toto, T. T.; de Melo, C. P. *Chem. Phys. Lett.* **1995**, *245*, 660. Toto, J. L.; Toto, T. T.; de Melo, C. P.; Robins, K. A. *J. Chem. Phys.* **1995**, *102*, 8048. Albert, I. D. L.; Marks, T. J.; Ratner, M. A. In *Nonlinear Optical Materials, Theory and Modeling*; Karna, S. P., Yeates, A. T., Eds.; ACS Symposium Series; American Chemical Society: Washington, DC, 1995; Vol. 628, p 116. Sekino, H.; Bartlett, R. J. *Chem. Phys. Lett.* **1995**, *234*, 87. Nakano, M.; Kiribayashi, S.; Yamada, S.; Shigemoto, I.; Yamaguchi, K. *Chem. Phys. Lett.* **1996**, *262*. Champagne, B.; Mosley, D. H. *J. Chem. Phys.* **1996**, *105*, 3592. Jacquemin, D.; Champagne, B.; André, J. M. *Int. J. Quantum Chem.* **1997**, *65*, 679. Jacquemin, D.; Champagne, B.; André, J. M. *Chem. Phys. Lett.* **1998**, *284*, 24. Nakano, M.; Yamada, S.; Kiribayashi, S.; Yamaguchi, K. *Int. J. Quantum Chem.* **1998**, *70*, 269. Kamada, K.; Ueda, M.; Nagao, H.; Tawa, K.; Sugino, T.; Shimizu, Y.; Ohta, K. *Int. J. Quantum Chem.* **1998**, *70*, 737. Maroulis, G. *J. Chem. Phys.* **1999**, *111*, 583.

(2) Champagne, B.; Perpète, E. A.; van Gisbergen, S. J. A.; Baerends, E. J.; Snijders, J. G.; Soubra-Ghaoui, C.; Robins, K. A.; Kirtman, B. *J. Chem. Phys*. **1998**, *109*, 10489.

(3) van Gisbergen, S. J. A.; Schipper, P. R. T.; Gritsenko, O. V.; Baerends, E. J.; Snijders, J. G.; Champagne, B.; Kirtman, B. *Phys. Rev. Lett.* **1999**, *83*, 694.

(4) Champagne, B.; Perpète, E. A. *Int. J. Quantum Chem*. **1999**, *75*, 441.

(5) Zangwill, A. *J. Chem. Phys*. **1983**, *78*, 5926.

(6) Senatore, G.; Subbaswamy, K. R. *Phys. Rev. A* **1986**, *34*, 3619; **1987**, *35*, 2440.

(7) Moullet, I.; Martins, J. L *J. Chem. Phys*. **1990**, *92*, 527.

(8) Jasien, P. G.; Fitzgerald, G. *J. Chem. Phys*. **1990**, *93*, 2554.

(9) Sim, F.; Salahub, D. R.; Chin, S. *Int. J. Quantum Chem.* **1992**, *43*, 463.

(10) Matsuzawa, N.; Dixon, D. A. *J. Phys. Chem.* **1992**, *96*, 6872.

(11) Guan, J.; Duffy, P.; Carter, J. T.; Chong, D. P.; Casida, K. C.; Casida, M. E.; Wrinn, M. *J. Chem. Phys.* **1993**, *98*, 4753.

(12) Colwell, S. M.; Murray, C. W.; Handy, N. C.; Amos, R. D. *Chem. Phys. Lett.* **1993**, *210*, 261.

(13) Lee, A. M.; Colwell, S. M. *J. Chem. Phys.* **1994**, *101*, 9704.

(14) Matsuzawa, N.; Dixon, D. A. *J. Phys. Chem.* **1994**, *98*, 2545.

(15) Dixon, D. A.; Matsuzawa, M. *J. Phys. Chem.* **1994**, *98*, 3967.

(16) Matsuzawa, N.; Dixon, D. A. *J. Phys. Chem.* **1994**, *98*, 11677.

(17) Dixon, D. A.; Chase, B. E.; Fitzgerald, G.; Matsuzawa, N. *J. Phys. Chem.* **1995**, *99*, 4486.

(18) Matsuzawa, N.; Dixon, D. A. *Synth. Met.* **1995**, *71*, 1667.

(19) McDowell, S. A. C.; Amos, R. D.; Handy, N. C. *Chem. Phys. Lett.* **1995**, *235*, 4.

(20) van Gisbergen, S. J. A.; Snijders, J. G.; Baerends, E. J. *J. Chem. Phys.* **1995**, *103*, 9347.

(21) Colwell, S. M.; Handy, N. C.; Lee, A. M. *Phys. Rev. A* **1996**, *53*, 1316.

(22) Jamorski, C.; Casida, M. E.; Salahub, D. R. *J. Chem. Phys.* **1996**, *104*, 5134.

(23) van Gisbergen, S. J. A.; Osinga, V. P.; Gritsenko, O. V.; van Leeuwen, R.; Snijders, J. G.; Baerends, E. J. *J. Chem. Phys.* **1996**, *105*, 3142.

(24) Dunlap, B. I.; Karna, S. P. In *Theoretical and Computational Modeling of NLO and Electronic Materials*; Karna, S. P., Yeates, A. T., Eds.; ACS Symposium Series; American Chemical Society: Washington, DC, 1996; Vol. 628, p 164.

(25) Dickson, R. M.; Becke, A. D. *J. Phys. Chem.* **1996**, *100*, 16105.

(26) Fuentealba, P.; Simón-Manson, Y. *J. Phys. Chem.* **1997**, *100*, 44231.

(27) Ioannou, A. G.; Colwell, S. M.; Amos, R. D. *Chem. Phys. Lett.* **1997**, *278*, 278.

(28) van Gisbergen, S. J. A.; Snijders, J. G.; Baerends, E. J. *Phys. Rev. Lett.* **1997**, *78*, 3097.

(29) van Gisbergen, S. J. A.; Kootstra, F.; Schipper, P. R. T.; Gritsenko, O. V.; Snijders, J. G.; Baerends, E. J. *Phys. Rev. A* **1998**, *57*, 2556.

(30) Calaminici, P.; Jug, K.; Köster, A. M. *J. Chem. Phys.* **1998**, *109*, 7756.

(31) Tozer, D. J.; Handy, N. C. *J. Chem. Phys.* **1998**, *108*, 10180.

(32) van Gisbergen, S. J. A.; Snijders, J. G.; Baerends, E. J. *J. Chem. Phys.* **1998**, *109*, 10644; erratum **1999**, *111*, 6652.

(33) van Gisbergen, S. J. A.; Snijders, J. G.; Baerends, E. J. *J. Chem. Phys.* **1998**, *109*, 10657.

(34) Millefiori, S.; Alparone, A. *J. Mol. Struct.* (*THEOCHEM*) **1998**, *422*, 179; *ibidem* **1998**, *431*, 59.

(35) Görling, A.; Heinze, H. H.; Ruzankin, S. Ph.; Staufer, M.; Rösch, N. *J. Chem. Phys.* **1999**, *110*, 2785.

(36) Cohen, A. J.; Tatirungrotechai, Y. *Chem. Phys. Lett.* **1999**, *299*, 465.
(37) Cohen, A. J.; Handy, N. C.; Tozer, D. J. *Chem. Phys. Lett.* **1999**, *303*, 391.
(38) Adamo, C.; Cossi, M.; Scalmani, G.; Barone, V. *Chem. Phys. Lett.* **1999**, *307*, 265.
(39) Schipper, P. R. T.; Gritsenko, O. V.; van Gisbergen, S. J. A.; Baerends, E. J. *J. Chem. Phys.*, **2000**, *112*, 1344.
(40) van Leeuwen, R.; Baerends, E. J. *Phys. Rev. A* **1994**, *49*, 2421.
(41) Krieger, J. B.; Li, Y.; Iafrate, G. J. *Phys. Rev. A* **1992**, *45*, 101; **1993**, *47*, 165. Li, Y.; Krieger, J. B.; Norman, M. R.; Iafrate, G. J. *Phys. Rev. B* **1991**, *44*, 10437.
(42) Godby, R. W.; Sham, L. J. *Phys. Rev. B* **1994**, *49*, 1849. Aulbur, W. G.; Jönsson, L.; Wilkins, J. W. *Phys. Rev. B* **1996**, *54*, 8540.
(43) Parr, R. G.; Wang, W. *Density Functional Theory of Atoms and Molecules*; Oxford University Press: Oxford, UK, 1989.
(44) Baerends, E. J.; Gritsenko, O. V. *J. Phys. Chem.* **1997**, *101*, 5383.
(45) Slater, J. C. *Phys. Rev.* **1951**, *81*, 385.
(46) Vosko, S. J.; Wilk, L.; Nusair, M. *Can. J. Phys.* **1980**, *58*, 1200.
(47) Becke, A. D. *Phys. Rev. A* **1988**, *38*, 3098.
(48) Perdew, J. P.; Wang, Y. *Phys. Rev. B* **1992**, *45*, 13244.
(49) Gill, P. M. W. *Mol. Phys.* **1996**, *89*, 433.
(50) Lee, C.; Yang, W.; Parr, R. G. *Phys. Rev. B* **1988**, *37*, 785.
(51) Becke, A. D. *J. Chem. Phys.* **1993**, *98*, 5648.
(52) *GAUSSIAN94*; Frisch, M. J.; Trucks, G. W.; Schlegel, H. B.; Gill, P. M. W.; Johnson, B. G.; Robb, M. A.; Cheeseman, J. R.; Keith, T.; Peterson, G. A.; Montgomery, J. A.; Raghavachari, K.; Al-Laham, M. A.; Zakrzewski, V. G.; Ortiz, J. V.; Foresman, J. B.; Cioslowski, J.; Stefanov, B. B.; Nanayakkara, A.; Challacombe, M.; Peng, C. Y.; Ayala, P. Y.; Chen, W.; Wong, M. W.; Andres, J. L.; Replogle, E. S.; Gomperts, R.; Martin, R. L.; Fox, D. J.; Binkley, J. S.; DeFrees, D. J.; Baker, J.; Stewart, J. J. P.; Head-Gordon, M.; Gonzalez, C.; Pople, J. A. Gaussian Inc.: Pittsburgh, PA, 1995.
(53) *GAUSSIAN98*, Revision A.7; Frisch, M. J.; Trucks, G. W.; Schlegel, H. B.; Scuseria, G. E.; Robb, M. A.; Cheeseman, J. R.; Zakrzewski, V. G.; Montgomery, J. A.; Stratmann, R. E.; Burant, J. C.; Dapprich, S.; Millam, J. M.; Daniels, A. D.; Kudin, K. N.; Strain, M. C.; Farkas, O.; Tomasi, J.; Barone, V.; Cossi, M.; Cammi, R.; Mennucci, B.; Pomelli, C.; Adamo, C.; Clifford, S.; Ochterski, J.; Petersson, G. A.; Ayala, P. Y.; Cui, Q.; Morokuma, K.; Malick, D. K.; Rabuck, A. D.; Raghavachari, K.; Foresman, J. B.; Cioslowski, J.; Ortiz, J. V.; Stefanov, B. B.; Liu, G.; Liashenko, A. P.; Piskorz, A. P.; Komaromi, I.; Gomperts, R.; Martin, R. L.; Fox, D. J.; Keith, T.; Al-Laham, M. A.; Peng, C. Y.; Nanayakkara, A.; Gonzalez, C.; Challacombe, M.; Gill, P. M. W.; Johnson, B. G.; Chen, W.; Wong, M. W.; Andres, J. L.; Head-Gordon, M.; Replogle, E. S.; Pople, J. A. Gaussian Inc.: Pittsburgh, PA, 1998.
(54) Adamo, C.; Barone, V. *J. Chem. Phys.* **1998**, *108*, 664.
(55) van Gisbergen, S. J. A.; Snijders, J. G.; Baerends, E. J. *Comput. Phys. Commun.* **1999**, *118*, 119.
(56) ADF 1999; Baerends, E. J.; Bérces, A.; Bo, C.; Boerrigter, P. M.; Cavallo, L.; Deng, L.; Dickson, R. M.; Ellis, D. E.; Fan, L.; Fischer, T. H.; Fonseca Guerra, C.; van Gisbergen, S. J. A.; Groeneveld, J. A.; Gritsenko, O. V.; Harris, F. E.; van den Hoek, P.; Jacobsen, H.; van Kessel, G.; Kootstra, F.; van Lenthe, E.; Osinga, V. P.; Philipsen, P. H. T.; Post, D.; Pye, C. C.; Ravenek, W.; Ros, P.; Schipper, P. R. T.; Schreckenbach, G.; Snijders, J. G.; Sola, M.; Swerhone, D.; te Velde, G.; Vernooijs, P.; Versluis, L.; Visser, O.; van Wezenbeek, E.; Wiesenekker, G.; Wolff, S. K.; Woo, T. K.; Ziegler, T.. Fonseca Guerra, C.; Snijders, J. G.; te Velde, G.; Baerends, E. J. *Theor. Chem. Acc.* **1998**, *99*, 391.
(57) Perdew, J. P. *Phys. Rev. B* **1986**, *33*, 8822.
(58) Kirtman, B.; Champagne, B. *Int. Rev. Phys. Chem.* **1997**, *16*, 389. Champagne, B.; Kirtman, B. *Chem. Phys.* **1999**, *245*, 213.
(59) See for instance, Fournier, R.; Andzelm, J.; Salahub, D. R. *J. Chem. Phys.* **1989**, *90*, 6371. Komornicki, A.; Fitzgerald, G. *J. Chem. Phys.* **1993**, *98*, 1398.
(60) Gross, E. K. U.; Dobson, J. F.; Petersilka, M. In *Density Functional Theory*; Nalewajski, R. F., Ed.; Topics in Current Chemistry; Springer: Heidelberg, Germany, 1996.
(61) Davis, P. J.; Rabinowitz, P. *Numerical Integration*; Blaisdell Publishing Co.: London, 1967; 166.
(62) For example, see: Langhoff, P. W.; Karplus, M.; Hurst, R. P. *J. Chem. Phys.* **1966**, *44*, 505; Caves, T. C.; Karplus, M. *J. Chem. Phys.* **1969**, *50*, 3649. Dykstra, C. E.; Jasien, P. G. *Chem. Phys. Lett.* **1984**, *109*, 388. Sekino, H.; Bartlett, R. J. *J. Chem. Phys.* **1986**, *85*, 976. Karna, S. P.; Dupuis, M. *J. Comput. Chem.* **1991**, *12*, 487.
(63) Hehre, W. J.; Ditchfield, R.; Pople, J. A. *J. Chem. Phys.* **1972**, *56*, 2257.
(64) Hurst, G. J. B.; Dupuis, M.; Clementi, E. *J. Chem. Phys.* **1988**, *89*, 385. Perez, J.; Dupuis, M. *J. Phys. Chem.* **1991**, *95*, 6525.
(65) Jacquemin, D.; Champagne, B.; Hättig, C. *Chem. Phys. Lett.* **2000**, *319*, 327.
(66) Basis and fit sets are available on-line at http://www.scm.com/Doc/atomicdata.
(67) Jacquemin, D.; Champagne, B.; Perpète, E. A. P.; Luis, J. M.; Kirtman, B., manuscript in preparation.
(68) Jacquemin, D., unpublished work.
(69) Sim, F.; Chin, S.; Dupuis, M.; Rice, J. E. *J. Phys. Chem.* **1993**, *97*, 1158.
(70) Tretiak, S.; Chernyak, V.; Mukamel, S. *Chem. Phys. Lett.* **1998**, *287*, 75.
(71) Kirtman, B.; Champagne, B.; Bishop, D. M., submitted for publication. The restriction to qualitative aspects involves the fact that the amplitude of this field depends on chain length as well as upon the property.